https://dx.doi.org/10.1016/j.istruc.2018.11.011

Resistance of axially loaded hot-finished S460 and S690 steel square hollow stub columns at elevated temperatures

Han Fang[a] and Tak-Ming Chan[a,*]

[a]Department of Civil and Environmental Engineering, The Hong Kong Polytechnic University, Hung Hom, Hong Kong, China

Abstract

The resistance of axially-loaded hot-finished S460 and S690 steel square hollow stub columns at elevated temperatures was investigated in this study through finite element modelling. Finite element models were developed and validated against test results on hot-finished S460 and S690 steel square hollow stub columns under axial compressive loading. Extensive parametric studies were subsequently carried out to examine the axial compressive resistance of hot-finished S460 and S690 steel square hollow stub columns with a wide range of cross-sectional slenderness and at elevated temperatures up to 700°C. The results from parametric studies were compared with the strength predictions estimated based on design rules from European and American standards and the direct strength method. The reliability of these design rules for the structures subject to elevated temperatures was also evaluated through the reliability analysis. The comparison between parametric studies results and strength predictions shows that the design rules from European and American standards underestimate the strengths of the stub columns while the direct strength method provides quite accurate strength predictions for stub columns. Modified design rules were also found to provide safe and reliable strength predictions and can be used for structural design.

Keywords: Hot-finished, S460, S690 steel, square hollow stub columns, finite element modelling, elevated temperatures, design

1. Introduction

High strength steel (HSS) with nominal yield strength of at least 460MPa has become an attractive construction material for different structural applications. Using high strength steel allows to reduce the structural element sizes and subsequently brings about advantages including savings of weight consumption of construction materials, lower transportation costs and easier handling during construction. In order to conduct safe and economical design of HSS structures, extensive research studies on the hot-finished HSS structures and the HSS structures fabricated through welding and

cold-forming have been conducted to measure the material properties and residual stresses of the structures [1-4] and to examine the behaviour of the structures subject to compression [3, 5-7], bending [8-9] and combinations of compression and bending [10-11] at room temperature. Based on the results of these studies, design recommendations were proposed [12-15]. However, the structures also need to be designed for the possibility of fire exposure during which the structures experience strength deterioration due to the variation of material properties of steel [16-18] at elevated temperatures in fire [19].

Research studies have been conducted to examine the performance of HSS structural members at elevated temperatures. Chen and Young [20] investigated the strengths of BISALLOY 80 high strength steel (with the nominal yield strength of 690 MPa) stub and long columns with stocky box and I- sections at elevated temperatures through numerical modelling. It was also found that the design rules given in European and American standards and direct strength method [21] can be used to conservatively predict the column strengths. Fang and Chan [22] also performed numerical investigations on the welded S460 steel stub and long columns at elevated temperatures, covering the columns with stocky and slender box and H-sections. This study also shows that existing design rules in European and American standards provide unduly conservative strength predictions for the columns at various elevated temperatures while the direct strength method overestimates the strengths of columns with slender box and H-sections. The investigations and results in the above studies reveal that the understanding into the structural performance of hot-finished HSS columns with a wide range of cross-sectional slenderness and different steel grades is limited. The applicability of existing design rules for hot-finished S460 and S690 columns especially with slender cross-sections at elevated temperatures remains undetermined. Accurate design rules for the structures are also needed in order to achieve safe and economical structural design.

In this study, the axial compressive strengths of hot-finished S460 and S690 steel square hollow sections at elevated temperatures were investigated using finite element modelling. Reduced mechanical properties at elevated temperatures were used in the modelling. The investigations covered the square hollow sections with a wide range of cross-sectional slenderness and subject to varying elevated temperatures from room temperature up to 700^{o}C. Based on the resultant column strengths, the accuracy and reliability of design rules in European and American standards [23-24] and direct strength method were evaluated. Design recommendations were also discussed.

2. FE models and validation

Finite element (FE) models for hot-finished S460 and S690 steel square hollow sections under axial compression were developed using the software package ABAQUS 6.14 [25]. The FE models were validated against the experimental results for the structures under room temperature condition [3]. The

FE models and their validation are illustrated in the following sections. Subsequent parametric studies were carried out by replacing the material properties at room temperature with the properties at elevated temperatures, as introduced in Section 3.

2.1 Description of FE models

The element type chosen to simulate the S460 and S690 steel square hollow sections under axial compression was the four-noded shell element S4R with reduced integration. This element has been successfully applied to accurately predict the behaviour of HSS hollow members [13, 26]. The mesh size equal to the cross-sectional plate thickness was adopted for the FE models by conducting a mesh sensitivity study. The measured material properties for the tested square hollow section stub columns [3] were used for the modelling. Measured stress-strain curves reported in the experimental investigations were converted into the true stress and logarithmic plastic true strain curves which were incorporated in the FE models.

Residual stresses may exist in the steel hollow sections and can lead to reductions in the load carrying capacity of the structures. Residual stresses were measured for the hot-finished S460 and S690 steel square hollow sections by Wang et al. [9]. The results in the study show that the residual stresses in the sections are quite low and below 5.5% of the material yield strength. Due to the low magnitudes, the effect of residual stresses on the performance of hot-finished S460 and S690 steel square hollow section structures has also been found to be quite limited [9, 26]. Therefore, the incorporation of residual stresses was unnecessary.

The fixed-ended boundary conditions applied to the steel hollow section stub columns in the tests were also replicated in the FE models. Two reference points were developed and coupled with the nodes of end surfaces of each hollow section. All degrees of freedom of the reference points were restrained except for the longitudinal translation of the reference point at the loaded end. The axial compressive load was applied in a Riks step of each FE model by specifying a longitudinal displacement at the reference point on the loaded side. The modified Riks method [22, 27-28] was employed to trace the load-displacement behaviour of each steel square hollow section stub column.

Initial local geometric imperfections also exist in the hot-finished S460 and S690 steel square hollow sections and can influence the load-carrying capacity of the sections. Therefore, the local geometric imperfections were also incorporated for each section in the form of the lowest elastic local buckling mode shape, obtained by performing a prior eigenvalue buckling analysis. The buckling mode pattern was factored by the local geometric imperfection amplitudes for the FE models. Four amplitudes were used, including the measured amplitude (ω_0), 1/20 of the cross-sectional plate thickness, 1/100 of the cross-sectional plate thickness and the imperfection amplitude ($\omega_{D\&W}$) calculated from Eq. (1)

proposed by Gardner et al. [29] for hot-finished square hollow sections based on the Dawson and Walker (D&W) model [30]. In Eq. (1), f_y is the material yield strength, f_{cr} is the elastic critical buckling stress of the most slender plate element in a cross-section and t is the plate thickness.

$$\omega_{D\&W} = 0.028\left(f_y/f_{cr}\right)^{0.5} \times t \quad (1)$$

2.2 Validation

The FE models were compared against the test results [3] of hot-finished S460 and S690 steel square hollow section stub columns which are presented in Table 1. The stub column labels in the table are based on the steel grade and the dimensions of the stub columns. For example, the label "SHS460-50×5" defines the following stub column: SHS refers to the square hollow section, the digits "460" represent the steel grade of S460 and the term "50×5" indicates the nominal width and plate thickness of the section.

The ultimate compressive loads estimated based on different local geometric imperfection amplitudes were compared with the experimental results, as shown in Table 1. It can be observed that the ultimate compressive loads were accurately predicted using the measured local geometric imperfection amplitudes (ω_0). The predictions using the amplitudes ($\omega_{D\&W}$) calculated from Eq. (1) also compared well with the experimental results and are more accurate and less scattered than the predictions using the amplitudes of 1/20 and 1/100 of the cross-sectional plate thickness. The load-end shortening curves obtained from FE modelling were also compared with the experimental results for typical stub columns, as displayed in Fig. 1. The comparison of failure modes obtained from FE modelling with those from experiments is presented in Figs. 2 and 3. As can be seen in these figures, excellent agreement was obtained between the experimental and FE results. Therefore, the FE models are validated to be capable of accurately replicating the experimental results for hot-finished S460 and S690 steel square hollow sections under axial compression.

3. Parametric studies

Having the FE models validated for the hot-finished S460 and S690 steel square hollow section stub columns, parametric studies on 126 stub columns were conducted to obtain further data of the axial compressive resistance of the structures with a wide range of cross-sectional slenderness and subject to various elevated temperatures. The dimensions of the cross-sections for parametric studies are provided in Table 2, covering both stocky and slender cross-sections according to the cross-section classification specifications based on Eurocode 3 [3, 23]. The length of the stub columns was taken as three times of the cross-sectional width. This arrangement is consistent with that used for the

experimental investigations [3]. The stub columns with the dimensions shown in Table 2 were investigated at nine different temperatures including room temperature, 300°C, 400°C, 450°C, 500°C, 550°C, 600°C, 650°C and 700°C by using the material properties at these temperatures. The temperature distribution in the stub columns is considered to be uniform at each temperature. For S460 stub columns, the material stress-strain properties at elevated temperatures were obtained using the stress-strain curve model proposed by Fang and Chan [22] based on the average material properties measured by Wang et al. [3] and reduction factors based on the study of Qiang et al. [31] for S460 steel at elevated temperatures. The stress-strain model for S460 steel [22] is given as Eqs. (2)-(5) in which ε_T is the strain at temperature T, f_T is the stress at temperature T, E_T is the elastic modulus at temperature T, $f_{0.2,T}$ is the 0.2% proof stress at temperature T, $f_{u,T}$ is the ultimate stress at temperature T, $\varepsilon_{0.2,T}$ is the strain when the stress is $f_{0.2,T}$ at temperature T and T is the temperature degree in Celsius (°C). As for S690 stub columns, the stress-strain curve model proposed by Chen and Young [20] and given in Eqs. (2)-(6) were employed to obtain the material stress-strain properties using the average material properties measured by Wang et al. [3] and reduction factors obtained from the study of Qiang et al. [32] for S690 steel at elevated temperatures. In Eqs. (3) and (6), $E_{y,T}$ is the elastic modulus at 0.2% proof stress at temperature T. The reduction factor values for material properties at different temperatures are provided in Tables 3 and 4 for S460 and S690 respectively. Local geometric imperfections were also incorporated in the modelling for the stub columns at different temperatures, following the arrangements introduced in Section 2.1. Since the FE results based on the local geometric imperfection amplitudes ($\omega_{D\&W}$) agreed well with the experimental results, the $\omega_{D\&W}$ values estimated using Eq. (1) were adopted for modelling the stub columns given in Table 2 in the parametric studies.

$$\varepsilon_T = \frac{f_T}{E_T} + 0.002\left(\frac{f_T}{f_{0.2,T}}\right)^{n_0}, for\ S460\ and\ S690\ when\ f_T \le f_{0.2,T} \tag{2}$$

$$\varepsilon_T = \begin{cases} \frac{f_T - f_{0.2,T}}{E_T} + \varepsilon_{u,T}\left(\frac{f_T - f_{0.2,T}}{f_{u,T} - f_{0.2,T}}\right)^{n_1} + \varepsilon_{0.2,T}, for\ S460 \\ \frac{f_T - f_{0.2,T}}{E_{y,T}} + \varepsilon_{u,T}\left(\frac{f_T - f_{0.2,T}}{f_{u,T} - f_{0.2,T}}\right)^{n_1} + \varepsilon_{0.2,T}, for\ S690 \end{cases}, \ when\ f_T > f_{0.2,T} \tag{3}$$

$$n_0 = \begin{cases} 12 - \frac{T}{100}, for\ S460 \\ 7 - \frac{T}{250}, for\ S690 \end{cases} \tag{4}$$

$$n_1 = \begin{cases} 2.1 + \frac{3T}{1000}, for\ S460 \\ 1.6 + \frac{T}{600}, for\ S690 \end{cases} \tag{5}$$

$$E_{y,T} = \frac{E_T}{1 + 0.002 n_0 E_T / f_{0.2,T}} \tag{6}$$

4. Design rules

Three design rules including the Eurocode 3: part 1-2 [23], AISC 360 [24] and direct strength method are introduced in this section and their applicability to hot-finished S460 and S690 steel square hollow section stub columns at elevated temperatures was evaluated by comparing the strength predictions based on these design rules with the parametric studies results and performing the reliability analysis. The dimensions and material properties for the parametric studies were used to obtain the design predictions. According to Eurocode 3: part 1-2 [23], the yield stress ($f_{y,T}$) for stub columns with stocky (Class 1-3) cross-sections at elevated temperatures should be taken as the stress at 2% strain ($f_{2.0,T}$) while the yield stress ($f_{y,T}$) for stub columns with slender (Class 4) cross-sections at elevated temperatures should be taken as the 0.2% proof stress ($f_{0.2,T}$). Such arrangement was also employed for predicting the strengths of stub columns according to AISC 360 [24] and the direct strength method in order to directly compare the accuracy of different design rules for hot-finished S460 and S690 steel square hollow section stub columns at elevated temperatures.

4.1 Reliability analysis

The reliability of the aforementioned design rules can be examined through reliability analysis [33-34]. The reliability analysis was performed according to AISC 360 [24]. For each design rule, the reliability index (β) was calculated using Eq. (7). The design rule is regarded to be reliable when the value of β is greater than 2.6. The resistance factor (ϕ) values of 1.0, 0.9 and 0.85 were used for Eurocode 3: part 1-2, AISC 360 standard and the direct strength method [37]. The load combinations of 1.35DL (dead load)+1.5LL (live load) for Eurocode 3: part 1-2 [35] and 1.2DL+1.6LL for both AISC 360 and the direct strength method [36] were used for calculating the β values. The dead-to-live load ratio of 1/3 is specified for hot-rolled structural members [24, 26]. In Eq. (7), the statistical parameters M_m and V_m are the mean ratio of actual static yield stress over minimum specified yield stress and coefficient and variation (COV) of the yield strength [9]. The values of M_m and V_m equal to 1.12 and 0.0499 for S460 steel and 1.15 and 0.0605 for S690 steel were suggested by Wang et al. [9] and were employed to estimate β. The V_Q is the coefficient of variation of the load effect and was estimated to be 0.19. The parameters F_m=1.00 and V_F=0.02 are related to the uncertainty of geometric properties [9] while P_m and V_p are the mean value and COV for the experimental/FE-to-predicted strengths ratios. The ξ was estimated to be 0.692, 0.675 and 0.675 for Eurocode 3: part 1-2, AISC 360 standard and the direct strength method respectively.

$$\beta = \frac{\ln\left(\frac{M_m F_m P_m}{\xi \phi}\right)}{\sqrt{V_M^2 + V_F^2 + V_P^2 + V_Q^2}} \quad (7)$$

4.2 Evaluation of existing design rules using parametric studies results

4.2.1 European standard

Eurocode 3: part 1-2 [23] provides specifications for steel structural design at elevated temperatures. According to the standard, the strengths (N_{EC}) of stub columns at elevated temperatures can be calculated using Eqs. (8)-(12).

$$N_{EC} = \chi_{fi} * f_{y,T} * A_{eff} \quad (8)$$

$$\chi_{fi} = \frac{1}{\varphi_T + \sqrt{\varphi_T^2 - \bar{\lambda}_T^2}} \quad (9)$$

$$\varphi_T = 0.5 * (1 + \alpha\bar{\lambda}_T + \bar{\lambda}_T^2) \quad (10)$$

$$\bar{\lambda}_T = \bar{\lambda} * \left(k_{y,T}/k_{E,T}\right)^{0.5} \quad (11)$$

$$\alpha = 0.65 * \sqrt{235/f_{y,20}} \quad (12)$$

where A_{eff} is the effective cross-sectional area calculated using the material properties at room temperature according to Eurocode 3: part 1-5 [23, 38], χ_{fi} is the reduction factor, φ_T is the parameter to calculate χ_{fi} at temperature T, $k_{y,T}$ is the reduction factor for yield strength at temperature T, $k_{E,T}$ is the reduction factor for elastic modulus at temperature T, α is the imperfection factor and $\bar{\lambda}$ and $\bar{\lambda}_T$ are the non-dimensional slenderness at room and elevated temperature T respectively. The value of 0.65 in Eq. (12) is related to the severity factor [39].

The strengths N_{EC} calculated from Eqs. (8)-(12) were compared with the strengths (N_{FE}) of stub columns from parametric studies, as shown in Figs. 4 and 5 for S460 and S690 columns respectively. As can be seen in the figures, the strengths of hot-finished S460 and S690 steel square hollow section stub columns at elevated temperatures were underestimated. The mean value of N_{FE}/N_{EC} ratios for S460 steel square hollow section stub columns was estimated to be 1.07 with COV of 0.10 while the mean value of N_{FE}/N_{EC} ratios for S690 steel square hollow section stub columns was estimated to be 1.09 with COV of 0.06, as provided in Table 5. The reliability index (β) values were calculated for both S460 and S690 steel square hollow section stub columns, as shown in Table 5. It is shown in the table that the β value for S460 steel square hollow section stub columns equals to 2.48 and is below the target value of 2.6. Therefore, it is recommended that the resistance factor (ϕ) of 0.95 can be used. For the S690 steel square hollow section stub columns, the β value is 2.84 and higher than the target value when the ϕ equals to 1.0.

To improve the accuracy of strength predictions, Fang and Chan [22] proposed modifications to the design rule from Eurocode 3: part 1-2 for the welded S460 steel box and H-section stub and long columns. It has been suggested that the severity factor value of 0.3 can be used. The applicability of the modified design rule to hot-finished S460 and S690 stub columns was also evaluated. The strength predictions ($N^{\#}_{EC}$) calculated by replacing the value of 0.65 in Eq. (12) with the value of 0.3 were compared with the N_{FE}, as shown in Figs. 4 and 5 and Table 5. Comparing with the strength predictions based on original design rule, the accuracy of strength predictions was slightly improved by using the severity factor value of 0.3, as observed in Table 5. The β value for the modified Eurocode 3: part 1-2 design rule was found to be higher than the target value when the ϕ value of 0.95 was used for S460 steel stub columns. As for the S690 steel square hollow section stub columns, the β value is 2.80 and higher than the target value when the ϕ equals to 1.0.

4.2.2 American standard

The American standard AISC 360 [24] also provides specifications for estimating the cross-sectional strengths at elevated temperatures. According to AISC 360 standard, the strength of each stub column at any elevated temperature can be calculated based on the critical stress, as given as Eq. (13). In the equation, $P_{ne,T}$ is the compressive strength at temperature T ^{o}C, $F_{cr,T}$ is the critical stress at temperature T ^{o}C and A_g is the gross cross-sectional area. Eq. (14) is given in the standard for calculating the $F_{cr,T}$. In Eq. (14), the $f_{e,T}$ is the elastic buckling stress at temperature T ^{o}C.

$$P_{ne,T} = \begin{cases} F_{cr,T} * A_g, & for\ stocky\ cross-sections \\ F_{cr,T} * A_{eff}, & for\ slender\ cross-sections \end{cases} \quad (13)$$

$$F_{cr,T} = \left[0.42\sqrt{f_{y,T}/f_{e,T}}\right] f_{y,T} \quad (14)$$

The strength predictions for hot-finished S460 and S690 steel square hollow section stub columns at elevated temperatures based on AISC 360 standard were compared with the parametric studies results, as shown in Figs. 6 and 7. As can be seen in the figures, the predicted strengths (N_{AISC}) are much lower than the N_{FE} values obtained for the stub columns from parametric studies. The mean value of N_{FE}/N_{AISC} ratios for S460 steel square hollow section stub columns at elevated temperatures equals to 1.29 with COV of 0.11 while the mean value of N_{FE}/N_{AISC} ratios for S690 steel square hollow section stub columns at elevated temperatures equals to 1.27 with COV of 0.10, as provided in Table 5. The β values were also calculated to be 3.83 and 3.92 for S460 and S690 stub columns respectively. Therefore, the design rule in AISC 360 standard is reliable for the stub column structures.

The design rule from AISC 360 was modified by Fang and Chan [22] for welded S460 steel box and H-section columns to improve the accuracy of strength predictions for the structures. An equation was proposed in their study for calculating $F_{cr,T}$, as given as Eq. (15). Based on the $F_{cr,T}$ calculated from Eq. (15), the strengths ($N^{\#}_{AISC}$) predicted for hot-finished S460 and S690 steel square hollow section stub columns at elevated temperatures were compared with the N_{FE} values from parametric studies and the strengths (N_{AISC}) obtained based on the original design rule from AISC 360, as presented in Figs. 6 and 7 and Table 5. As can be seen from Figs. 6 and 7, the $N^{\#}_{AISC}$ values agree better with the N_{FE} for stub columns from parametric studies than the N_{AISC} values estimated based on the original design rule from AISC 360 standard. For S460 and S690 stub columns respectively, the mean values of $N_{FE}/N^{\#}_{AISC}$ equal to 1.07 and 1.05, with COV of 0.09 and 0.07 are compared with the mean values of N_{FE}/N_{AISC} equal to 1.29 and 1.27, with COV of 0.11 and 0.10. Therefore, the accuracy of strength predictions was obviously improved by using the $F_{cr,T}$ calculated from Eq. (15). The β values for the modified AISC 360 standard were estimated to be 3.13 and 3.24 for S460 and S690 stub columns respectively and are higher than the target value of 2.6.

$$F_{cr,T} = \left[0.65^{\left(f_{y,T}/f_{e,T}\right)}\right] f_{y,T} \tag{15}$$

4.2.3 Direct strength method

The direct strength method (DSM) was also evaluated for its applicability to hot-finished S460 and S690 steel square hollow section stub columns at elevated temperatures. According to the DSM, the strength of any stub column is estimated as the minimum of the strengths for global, local and distortional buckling. For the stub columns investigated in this paper, no global or distortional buckling was observed. Thus, the design equation for local buckling was used, as given as Eq. (16) [13, 21, 37]. In the equation, $P_{crl,T}$ is the critical elastic column local buckling load at temperature T while λ_l is the non-dimensional cross-section slenderness and equals to $(f_y A_g/P_{crl,T})^{0.5}$. The strengths ($N_{DSM}$) were estimated using the properties of S460 and S690 at elevated temperatures and were compared with the N_{FE} obtained for the stub columns from parametric studies in Figs. 8 and 9. A quantitative evaluation of the accuracy of strength predictions based on DSM was also performed. The mean values of N_{FE}/N_{DSM} ratios equal to 1.03 and 1.02 with the COV of 0.10 and 0.07 respectively for S460 and S690 stub columns, as shown in Table 5. For S460 and S690 stub columns respectively, the β values were calculated as 3.16 and 3.37, indicating that DSM is reliable for the structures.

$$N_{DSM} = \begin{cases} f_y * A_g, \ for\ \lambda_l \leq 0.776 \\ \left(1 - \frac{0.15}{\lambda_l^{0.8}}\right)\frac{1}{\lambda_l^{0.8}} f_y * A_g, \ for \lambda_l > 0.776 \end{cases} \tag{16}$$

The DSM was also modified by Fang and Chan [22] to provide safer strength predictions for welded S460 steel columns at elevated temperatures, as shown in Eq. (17). The comparison of strengths predicted ($N^{\#}_{DSM}$) using Eq. (17) with those from parametric studies and the strengths predicted using Eq. (16) is presented in Figs. 8 and 9. The curves of normalised N_{DSM} and $N^{\#}_{DSM}$ versus λ_l are also presented in Fig.10 in comparison with the results of parametric studies introduced in Section 3. The mean values for $N_{FE}/N^{\#}_{DSM}$ ratios for the stub columns are provided in Table 5. As can be seen in the table and Figs. 8-10, more conservative and less scattered strength predictions were obtained for the stub columns using the modified DSM [22]. The β values were found to be 3.52 and 3.78 for S460 and S690 stub columns respectively and are higher than the target value of 2.6.

$$N^{\#}_{DSM} = \begin{cases} f_y * A_g, \ for\ \lambda_l \leq 0.707 \\ \left(\frac{0.96}{\lambda_l^{0.9}} - \frac{0.22}{\lambda_l}\right) f_y * A_g, \ for \lambda_l > 0.707 \end{cases} \quad (17)$$

5. Conclusions

The structural performance of hot-finished S460 and S690 high strength steel stub columns at elevated temperatures was investigated. Finite element models were developed and validated against the experimental results for the stub columns. Extensive parametric studies were carried out for the stub columns with varying cross-sectional slenderness and subject to different elevated temperatures up to 700°C. The applicability of design rules in European and American standards and direct strength method for the stub columns at elevated temperatures was examined using the parametric studies results. The reliability of these design rules was also evaluated. The European standard was found to provide conservative strength predictions for hot-finished S460 and S690 high strength steel stub columns at elevated temperatures. The reliability requirement was unsatisfied for S460 steel stub columns while using the resistance factor specified as unity in the standard. Thus, the resistance factor value of 0.95 was proposed for S460 steel stub columns in order to achieve the reliability index to be higher than the target value. The modification to the design rule in European standard was proposed by Fang and Chan [22] and the modified design rule was also evaluated and found to provide more accurate strength predictions. The design rule from American standard provides the most conservative strength predictions than the predictions from other design rules for hot-finished S460 and S690 high strength steel stub columns at elevated temperatures. The modified design rule for American standard was proposed by Fang and Chan [22] and was found to provide more accurate strength predictions for the stub columns at elevated temperatures than the predictions based on original design rule in American standard. Both the original and modified design rule for American standard are reliable according to the reliability analysis results. The direct strength method was also examined. It provides quite accurate and reliable strength predictions for hot-finished S460 and S690 high strength steel stub columns at elevated temperatures. The modified direct strength method from Fang and Chan [22] was

also assessed for predicting the strengths for the stub columns. The modified direct strength method provides more conservative strength predictions than the original direct strength method and is reliable for hot-finished S460 and S690 high strength steel stub columns subject to elevated temperatures.

Acknowledgements

The authors are grateful for the support from the Chinese National Engineering Research Centre for Steel Construction (Hong Kong Branch) at The Hong Kong Polytechnic University.

References

[1] Ban, H.Y., Shi, G., Shi, Y.J. and Wang, Y.Q. 2013. Residual stress of 460 MPa high strength steel welded box section: Experimental investigation and modeling. *Thin-Walled Structures*, 64, 73-82.

[2] Ma, J.L., Chan, T.M. and Young, B. 2015. Material properties and residual stresses of cold-formed high strength steel hollow sections. *Journal of Constructional Steel Research*, 109, 152-165.

[3] Wang, J., Afshan, S., Schillo, N., Theofanous, M., Feldmann, M. and Gardner, L. 2017. Material properties and compressive local buckling response of high strength steel square and rectangular hollow sections. *Engineering Structures*, 130, 297-315.

[4] Fang, H., Chan, T.M. and Young, B. 2018. Material properties and residual stresses of octagonal high strength steel hollow sections. *Journal of Constructional Steel Research,* 148, 479-490.

[5] Ban, H.Y., Shi, G., Shi, Y.J. and Bradford, M.A. 2013. Experimental investigation of the overall buckling behaviour of 960 MPa high strength steel columns. *Journal of Constructional Steel Research*, 88, 256-266.

[6] Shi, G., Zhou, W.J. and Lin, C.C. 2015. Experimental investigation on the local buckling behaviour of 960MPa high strength steel welded section stub columns. *Advances in Structural Engineering*, 18, 423-437.

[7] Ma, J.L., Chan, T.M. and Young, B. 2016. Experimental investigation on stub-column behaviour of cold-formed high strength steel tubular sections. *Journal of Structural Engineering*, 142, 04015174.

[8] Ma, J.L., Chan, T.M. and Young, B. 2016. Experimental investigation of cold-formed high strength steel tubular beams. *Engineering Structures*, 126, 200-209.

[9] Wang, J., Afshan, S., Gkantou, M., Theofanous, M., Baniotopoulos, C. and Gardner, L. 2016. Flexural behaviour of hot-finished high strength steel square and rectangular hollow sections. *Journal of Constructional Steel Research*, 121, 97-109.

[10] Nie, S.D., Kang, S.B., Shen, L. and Yang, B. 2017. Experimental and numerical study on global buckling of Q460GJ steel box columns under eccentric compression. *Engineering Structures*, 142, 211-222.

[11] Ma, T.Y., Hu, Y.F., Liu, X., Li, G.Q. and Chung, K.F. 2017. Experimental investigation into high strength Q690 steel welded H-sections under combined compression and bending. *Journal of Constructional Steel Research*, 138, 449-462.

[12] Chan, T.M., Zhao, X.L. and Young, B. 2015. Cross-section classification for cold-formed and built-up high strength carbon and stainless steel tubes under compression. *Journal of Constructional Steel Research*, 106, 289-295.

[13] Ma, J.L., Chan, T.M. and Young, B. 2018. Design of cold-formed high strength steel tubular stub columns. *Journal of Structural Engineering*, 144(6), 04018063.

[14] Ban, H.Y. and Shi, G. 2018. Overall buckling behaviour and design of high-strength steel welded section columns. *Journal of Constructional Steel Research*, 143, 180-196.

[15] Ma, T.Y., Li, G.Q. and Chung, K.F. 2018. Numerical investigation into high strength Q690 steel columns of welded H-sections under combined compression and bending. *Journal of Constructional Steel Research*, 144, 119-134.

[16] Fang, H., Wong, M.B. and Yu, B. 2017. Heating rate effect on the thermophysical properties of steel in fire. *Journal of Constructional Steel Research*, 128, 611-617.

[17] Yang, K.C., Lee, H.H. and Chan, O. 2006. Experimental study of fire-resistant steel H-columns at elevated temperature. *Journal of Constructional Steel Research*, 62, 544-553.

[18] Takagi, J. and Deierlein, G.G. 2007. Strength design criteria for steel members at elevated temperatures. *Journal of Constructional Steel Research*, 63, 1036-1050.

[19] Wong, M.B. and Ghojel, J.I. 2003. Sensitivity analysis of heat transfer formulations for insulated structural steel components. *Fire safety Journal*, 38, 187-201.

[20] Chen, J. and Young, B. 2008. Design of high strength steel columns at elevated temperatures. *Journal of Constructional Steel Research*, 64, 689-703.

[21] Schafer, B.W. 2002. Local, distortional, and Euler buckling of thin-walled columns. *Journal of Structural Engineering*, ASCE, 128, 289-299.

[22] Fang, H. and Chan, T.M. 2018. Axial compressive strength of welded S460 steel columns at elevated temperatures. *Thin-walled Structures*, 129, 213-224.

[23] EN 1993-1-2, 2005. *Eurocode 3: Design of steel structures-Part 1-2: General rules-structural fire design*. Brussels: European Committee for Standardization.

[24] ANSI/AISC 360-16, 2016. *Specification for structural steel buildings*. AISC, Chicago.

[25] ABAQUS [Computer software] (2014). Dassault Systèmes, Providence, RI.

[26] Wang, J. and Gardner, L. 2017. Flexural buckling of hot-finished high-strength steel SHS and RHS columns. *Journal of Structural Engineering*, 143, 04017028.

[27] Crisfield, M.A. 1981. A fast incremental/iterative solution procedure that handles "snap-through". *Computers and Structures*, 13, 55-62.

[28] Ramm, E. 1981. Strategies for tracing the nonlinear response near limit points. *Non-linear Finite element analysis in Structural Mechanics*, 13, 63-89.

[29] Gardner, L., Saari, N. and Wang, F. 2010. Comparative experimental study of hot-rolled and cold-formed rectangular hollow sections. *Thin-Walled Structures*, 48, 495-507.

[30] Dawson, R.G. and Walker, A.C. 1972. Post-buckling of geometrically imperfect plates. *Journal of the Structural Division*, 98, 75-94.

[31] Qiang, X.H., Bijlaard, F.S.K. and Kolstein, H. 2013. Elevated-temperature mechanical properties of high strength structural steel S460N: experimental study and recommendations for fire-resistance design. *Fire Safety Journal*, 55, 15-21.

[32] Qiang, X.H., Bijlaard, F.S.K. and Kolstein, H. 2012. Dependence of mechanical properties of high strength steel S690 on elevated temperatures. *Construction and Building Materials*, 30, 73-79.

[33] Feng, R. and Young, B. 2012. Design of cold-formed stainless steel tubular joints at elevated temperatures. *Engineering Structures*, 35, 188-202.

[34] Huang, Y. and Young, B. 2018. Structural performance of cold-formed lean duplex stainless steel beams at elevated temperatures. *Thin-Walled Structures*, 129, 20-27.

[35] EN1990, 2002. *Eurocode — Basis of structural design*. Brussels: European Committee for Standardization.

393 [36] ASCE/SEI 7, 2016. *Minimum design loads for buildings and other structures*. ASCE, Reston,
394 VA.

395 [37] ANSI/AISI S100-16, 2016. *North American specification for the design of cold-formed steel*
396 *structural members*. AISI, Washington, DC.

397 [38] EN 1993-1-5, 2006. *Eurocode 3: Design of steel structures-Part 1-5: Plated structural elements*.
398 Brussels: European Committee for Standardization.

399 [39] Franssen, J.M., Talamona, D., Kruppa, J. and Cajot, L.G. 1998. Stability of steel columns in case
400 of fire: experimental evaluation. *Journal of Constructional Steel Research*, 124, 158-163.

Table 1. Comparison of stub column test results [3] with FE results using different imperfection amplitudes.

	Measured amplitude (ω_0)	**Plate thickness/20**	**Plate thickness/100**	**Dawson and Walker model ($\omega_{D\&W}$)**
Stub column	$N_{u,FE}/N_{u,test}$	$N_{u,FE}/N_{u,test}$	$N_{u,FE}/N_{u,test}$	$N_{u,FE}/N_{u,test}$
SHS460-50×5	0.98	0.89	0.98	0.98
SHS460-50×4	0.94	0.82	0.94	0.96
SHS460-100×5	0.99	0.97	0.99	0.99
SHS460-90×3.6	1.04	1.04	1.05	1.04
SHS690-50×5	0.97	0.95	0.97	0.97
SHS690-100×5.6	0.97	0.99	1.02	1.01
SHS690-90×5.6	1.03	1.00	1.07	1.07
Mean	0.99	0.95	1.00	1.00
COV	0.03	0.08	0.05	0.04

Table 2. Nominal cross-sectional dimensions of S460 and S690 stub columns for parametric studies.

Stub column cross-sections	Outer width B (mm)	Thickness t (mm)	Length (mm)
SHS50×5	50	5	150
SHS90×4.5	90	4.5	270
SHS90×4	90	4	270
SHS120×4.5	120	4.5	360
SHS120×4	120	4	360
SHS120×3	120	3	360
SHS120×2.5	120	2.5	360

Table 3. Reduction factors for material properties of S460 steel at different temperatures [31].

Temperature (ºC)	**Reduction factor**				
	E	**$f_{2.0}$**	**$f_{0.2}$**	**f_u**	**ε_u**
Room temperature	1	1	1	1	1
300	0.799	1	0.811	1	0.786
400	0.669	0.949	0.736	0.880	0.514
450	0.578	0.877	0.626	0.750	0.326
500	0.509	0.739	0.518	0.601	0.284
550	0.374	0.559	0.491	0.443	0.220
600	0.291	0.415	0.376	0.328	0.166
650	0.248	0.313	0.310	0.249	0.140
700	0.153	0.187	0.197	0.157	0.061

Table 4. Reduction factors for material properties of S690 steel at different temperatures [32].

Temperature (ºC)	**Reduction factor**				
	E	**$f_{2.0}$**	**$f_{0.2}$**	**f_u**	**ε_u**
Room temperature	1	1	1	1	1
300	0.839	0.975	0.879	0.961	0.685
400	0.775	0.850	0.794	0.828	0.303
450	0.730	0.737	0.711	0.748	0.250
500	0.685	0.624	0.628	0.668	0.198
550	0.546	0.533	0.554	0.558	0.191
600	0.372	0.371	0.380	0.377	0.171
650	0.257	0.252	0.240	0.254	0.195
700	0.141	0.133	0.100	0.130	0.220

Table 5. Comparison of the strengths from parametric studies with the predicted strengths based on different design rules for all stub columns at elevated temperatures.

Steel grade	**Parameters**	N_{FE}/N_{EC}	N_{FE}/N_{AISC}	N_{FE}/N_{DSM}	$N_{FE}/N^{\#}_{EC}$	$N_{FE}/N^{\#}_{AISC}$	$N_{FE}/N^{\#}_{DSM}$
S460	Mean	1.07	1.29	1.03	1.06	1.07	1.10
	COV	0.10	0.11	0.10	0.09	0.09	0.09
	ϕ	1	0.9	0.85	1	0.9	0.85
	β	2.48	3.83	3.16	2.49	3.13	3.52
	ϕ'	0.95	0.9	0.85	0.95	0.9	0.85
	β'	2.71	3.83	3.16	2.89	3.13	3.52
S690	Mean	1.09	1.27	1.02	1.08	1.05	1.10
	COV	0.06	0.10	0.07	0.06	0.07	0.06
	ϕ	1	0.9	0.85	1	0.9	0.85
	β	2.84	3.92	3.37	2.80	3.24	3.78

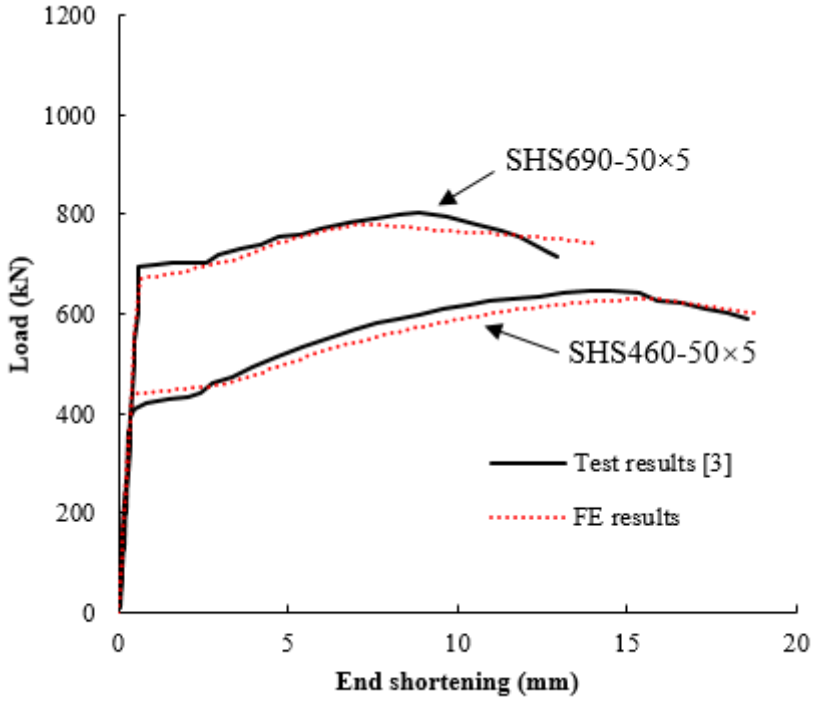

Figure 1. Experimental and FE results of load-end shortening curves for stub columns.

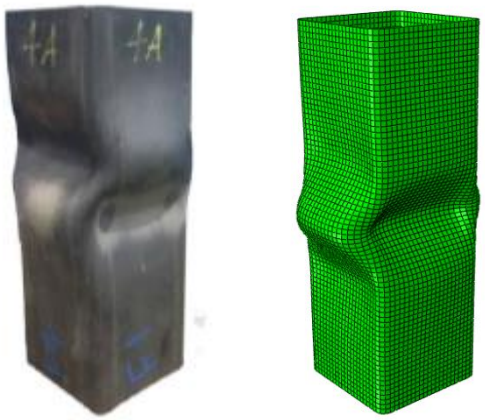

Figure 2. Comparison of the failure mode from experimental and FE results for SHS460-90×3.6 stub column [3].

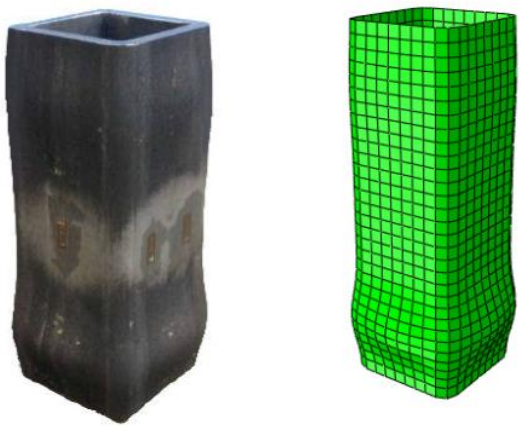

Figure 3. Comparison of the failure mode from experimental and FE results for SHS690-50×5 stub column [3].

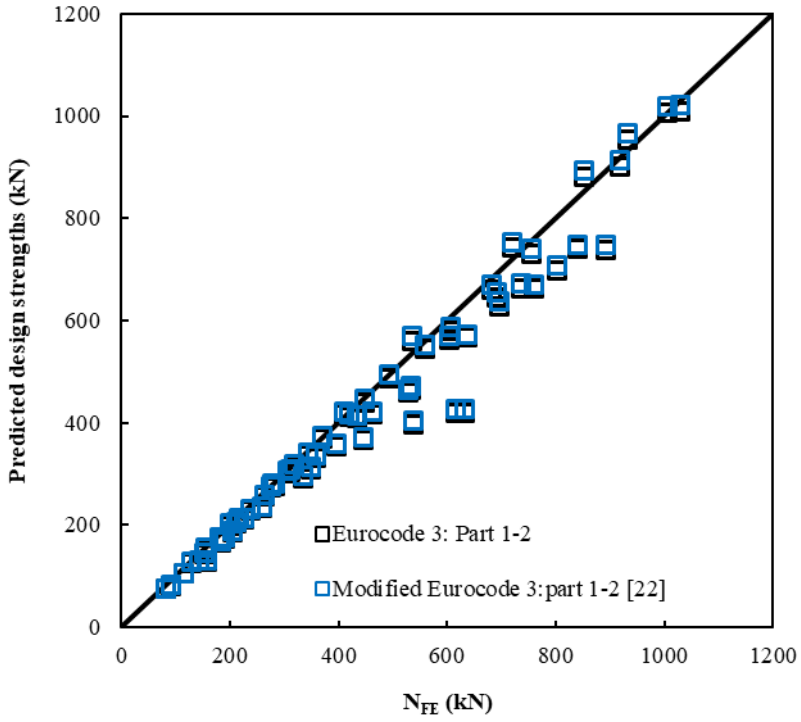

Figure 4. Comparison of strengths predicted based on European standard with FE results for S460 stub columns.

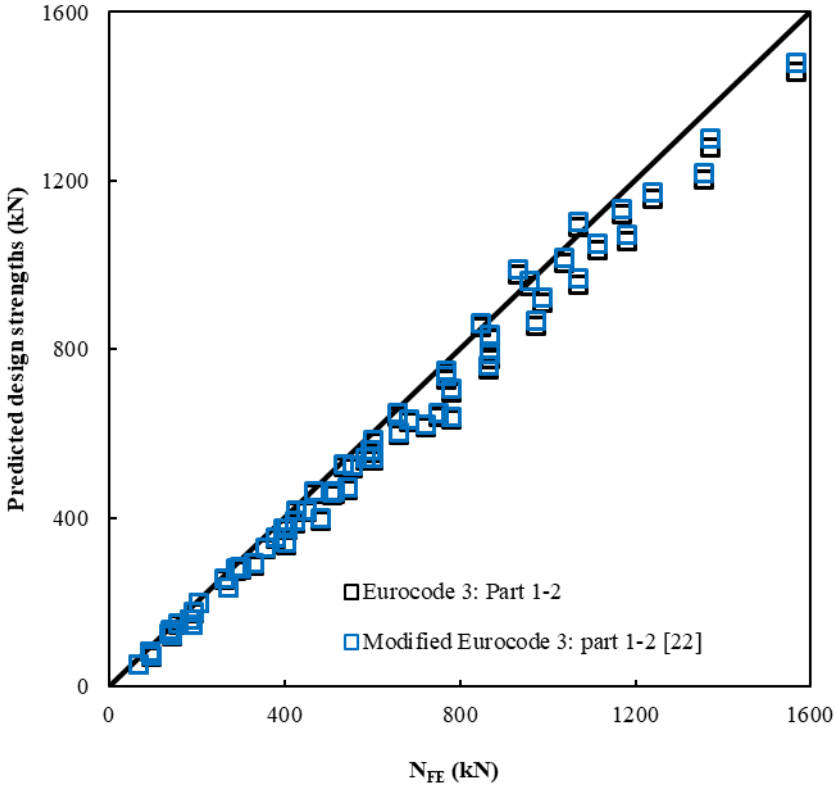

Figure 5. Comparison of strengths predicted based on European standard with FE results for S690 stub columns.

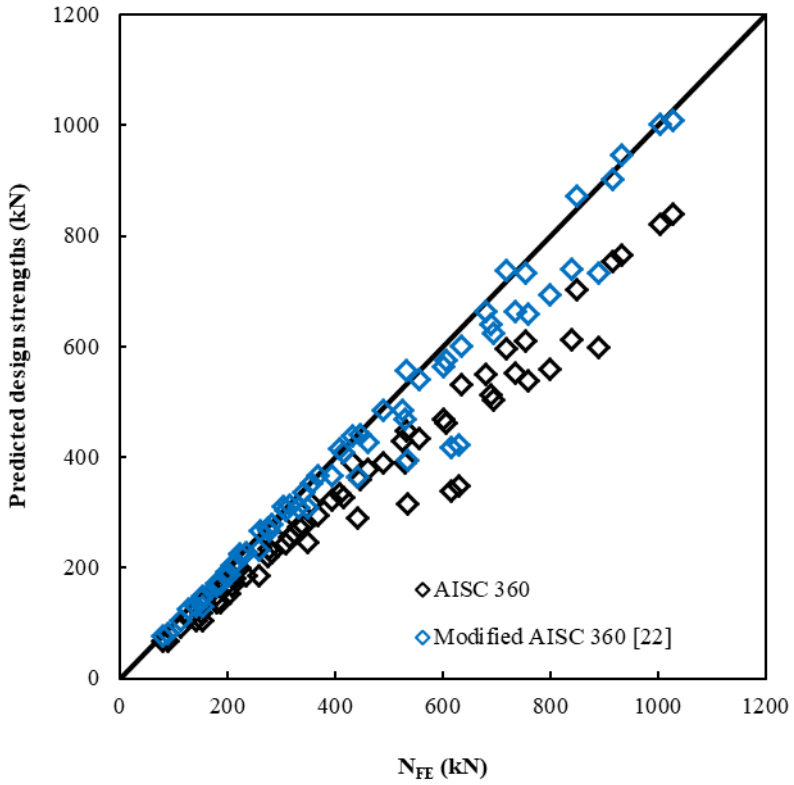

Figure 6. Comparison of strengths predicted based on AISC 360 standard with FE results for S460 stub columns.

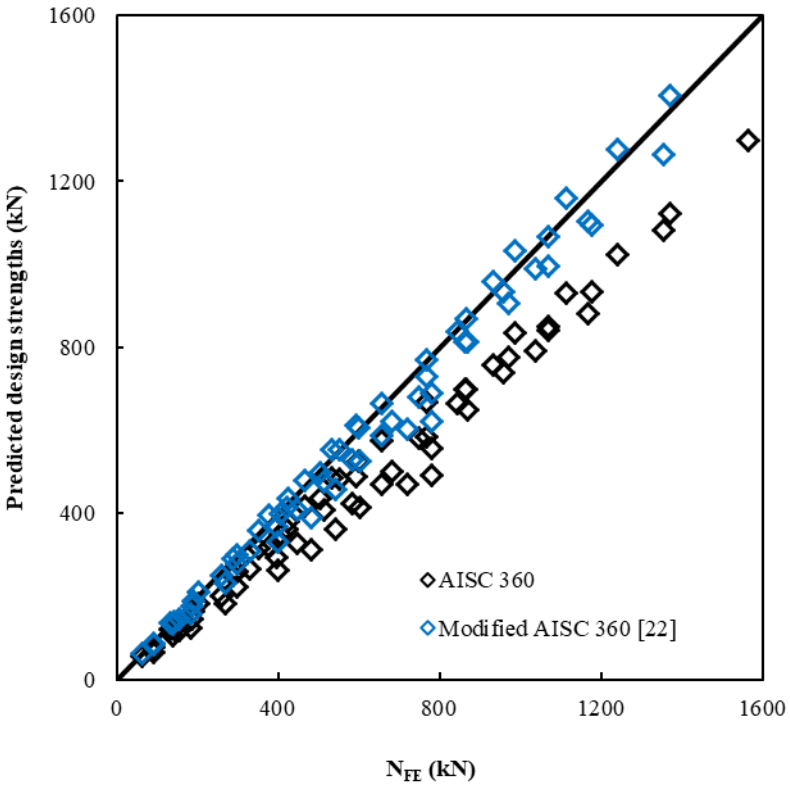

Figure 7. Comparison of strengths predicted based on AISC 360 standard with FE results for S690 stub columns.

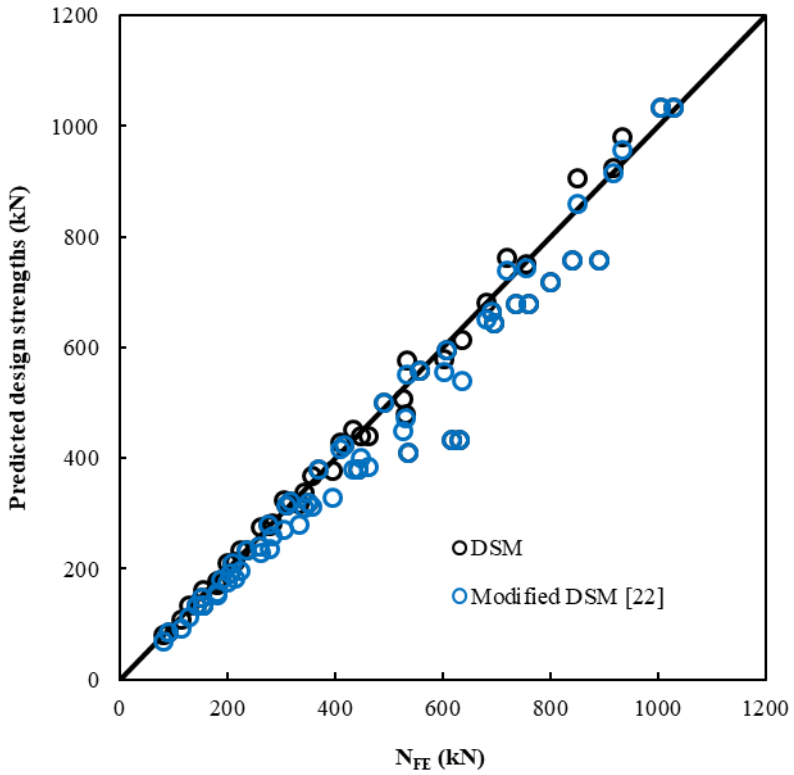

Figure 8. Comparison of strengths predicted based on DSM with FE results for S460 stub columns.

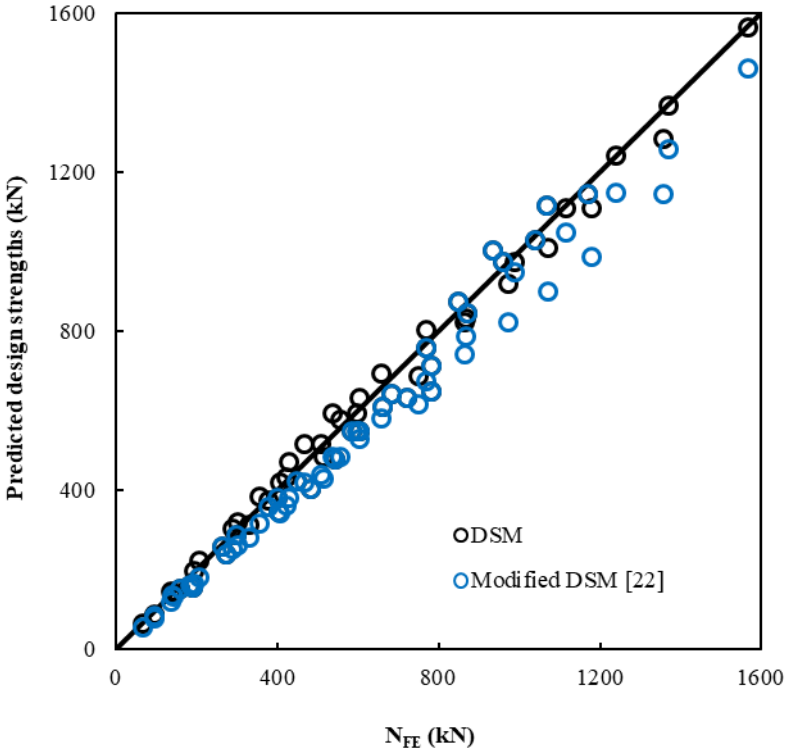

Figure 9. Comparison of strengths predicted based on DSM with FE results for S690 stub columns.

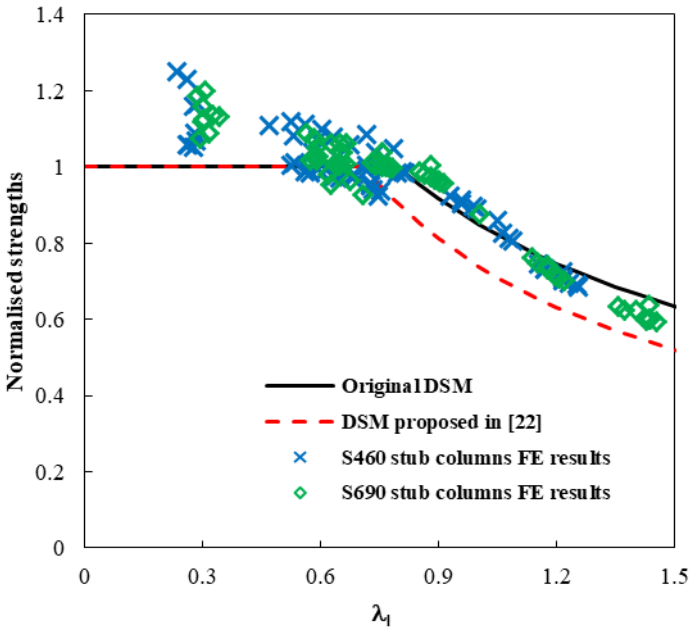

Figure 10. Comparison of the strengths from parametric studies and strength predictions based on both modified DSM approach and original DSM for stub columns.